Supplement for the paper

Trend in ice moistening the stratosphere – constraints from isotope data of water and methane

by:

Justus Notholt, Geoffrey C. Toon, Stephan Fueglistaler, Paul O. Wennberg, Fredrick W. Irion, Mike McCarthy, Marco Scharringhausen, Tae Siek Rhee, Armin Kleinböhl, and Voltaire Velazco

Balloon borne observations

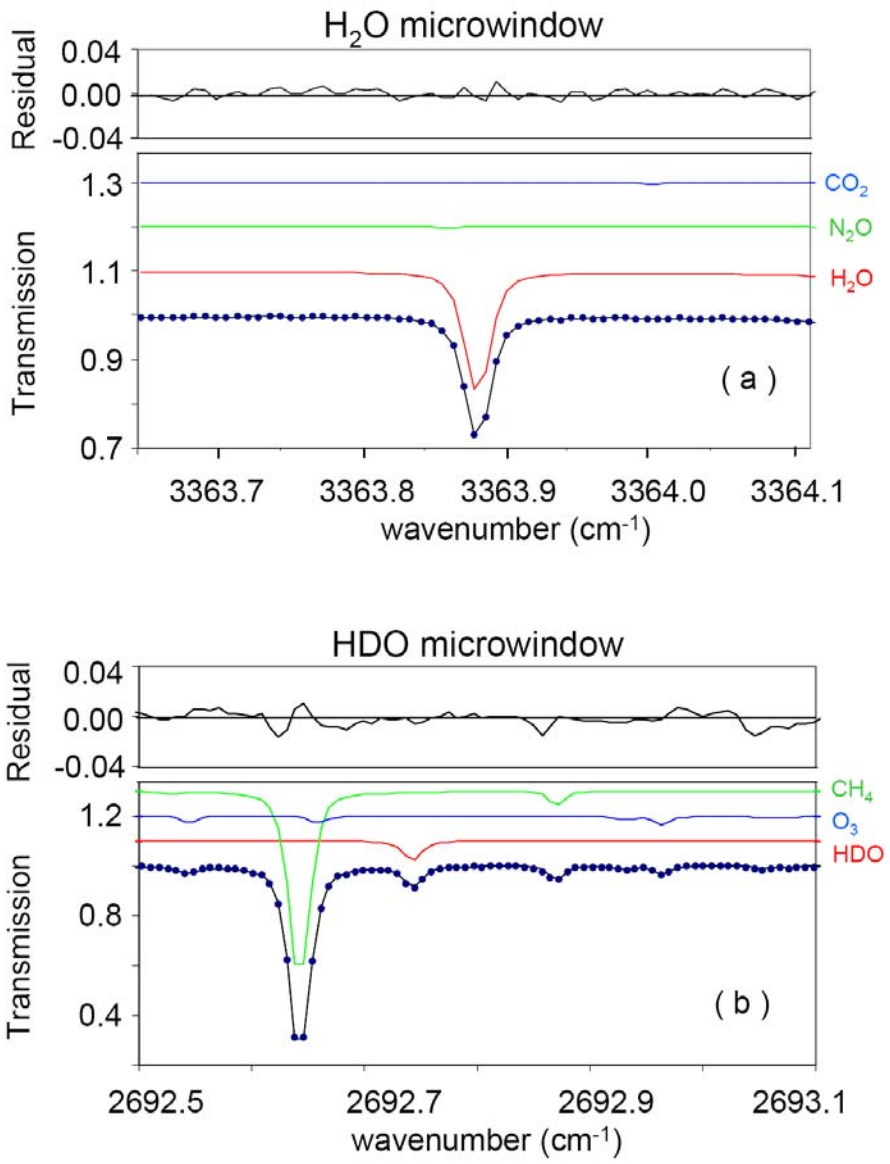

Figure. Examples for spectral microwindows covering isolated H_2O and HDO lines. The dark blue dots give the measured data, the dark blue line the corresponding best fit. The individual contributions by the trace gases (named on the right side) are given in red, green, and light blue. For clarity the individual contributions are shifted by 0.1. The residuals (measured minus simulated spectra) are given on top.

Uncertainty estimates

The total error in [H_2O^{entry}], [HDO^{entry}] or δD^{entry}, assuming Gaussian error propagation, is given by

$$\Delta f = \left(\sum_i \left(\frac{\partial f}{\partial x_i} \Delta x_i \right)^2 \right)^{1/2} \qquad (5)$$

For [H_2O^{entry}] this gives

$$\Delta[H_2O]^{entry} = \left(\Delta[H_2O]^2 - 4\,\Delta[CH_4]^2 \right)^{1/2} \qquad (6)$$

and for δD^{entry}

$$\Delta\delta D^{entry} = \left(\begin{array}{l} \left(\frac{\Delta[HDO]}{[H_2O]-2[CH_4]} \right)^2 + \left(\frac{\Delta[CH_3D]}{[H_2O]-2[CH_4]} \right)^2 \\ + \left(\frac{([HDO]-[CH_3D])\,\Delta[H_2O]}{([H_2O]-2[CH_4])^2} \right)^2 + \left(\frac{([HDO]-[CH_3D])\,\Delta[CH_4]}{([H_2O]-2[CH_4])^2} \right)^2 \end{array} \right)^{1/2} . \qquad (7)$$

For the average from different balloon launches and altitudes, the average and average error is given by

$$\langle f \rangle = \left(\sum_i \frac{f_i}{(\Delta x_i)^2} \right) \left(\sum_i \frac{1}{(\Delta x_i)^2} \right)^{-1} \qquad (8)$$

and $$\langle \Delta f \rangle = \left(\sum_i \frac{1}{(\Delta x_i)^2} \right)^{-1} \qquad (9)$$

No	year	day of year	Latitude (°)	Longitude (°)	sunrise/ sunset	Altitude range (km)
1	1991	126	35.6N-37.7N	106.7W-112.2W	sunset	39-15
2	1992	259	34.9N-35.2N	105.9W-111.1W	sunset	39-17
3	1992	260	35.3N-35.0N	103.9W-109.6W	sunrise	22-41
4	1993	94	34.3N-34.8N	110.3W-115.3W	sunset	17-38
5	1993	269	34.1N-33.9N	101.7W-109.8W	sunset	5-38
6	1993	270	33.2N-33.0N	94.3W-100.6W	sunrise	13-39
7	1994	143	34.3N-36.7N	103.7W-109.8W	sunset	37-13
8	1994	144	35.9N-33.0N	101.8W-108.9W	sunrise	13-39
9	1996	273	33.0N-32.7N	106.9W-116.3W	sunset	39-3
10	1997	128	70.6N-64.2N	144.8W-155.3W	sunrise	8-39
11	1997	189	64.8N-66.5N	147.3W-147.9W	sunrise	8-31
12	1997	190	66.2N-64.8N	148.2W-149.8W	sunset	31-9
13	1999	337	67.6N-62.5N	22.5E-15.6E	sunset	34-5
14	2000	75	67.7N-69.6N	37.8E-27.4E	sunrise	11-30
15	2002	350	63.5N-66.5N	32.4E-30.5E	sunrise	13-30
16	2003	91	69.2N-67.2N	39.9E-26.8E	sunrise	7-33
17	2003	263	34.3N-34.4N	107.7W-115.9W	sunset	37-5
18	2004	268	33.7N-33.8N	103.0W-111.1W	sunset	38-10
19	2005	264	34.9N-35.3N	107.7W-115.7W	sunset	38-11
20	2005	265	34.0N-33.9N	109.2W-114.3W	sunrise	15-30
21	2007	53	67.7N-67.5N	21.7E-22.0E	sunrise	25-34
22	2007	266	34.8N-34.7N	105.2W-112.3W	sunset	38-13
23	2007	267	34.6N-34.3N	99.3W-105.9W	sunrise	11-39

Table. Details for all balloon launches used in this study, giving the date, latitude, longitude, and altitude range of all measurements. Note that some flights have data for ascent and descent.